properties and also in modeling the transition probabilities. The Hall measurements involve the carrier concentration, and across-gap excitations depend on the details in the VBs and CB dispersions. These simulations and measurements require a detail description of the energy distribution of the free carriers.

II. THEORETICAL BACKGROUND

The parameterized electronic band structures (circles in Figs. 1 and 2) of $CuIn_{1-x}Ga_xSe_2$ are based on first-principles band structure calculation (solid lines in these figures) using the full-potential linearized augmented plane wave (FPLAPW) calculation.[18,19] The parameterization was optimized in Ref. 15, and the details of the parameterization as well as a discussion about the methods are presented in that work. Here, we focus on the exploring the DOS and the carrier concentration.

Throughout this work, the energies are referenced to the VB maximum. The longitudinal ∥ direction is along the (001) c-axis, and the transverse ⊥ direction is in the plane perpendicular to the longitudinal direction.

A. The density-of-states

The band-resolved DOS for the specific jth energy band is defined as

$$g_j(E) = \frac{1}{\Omega}\sum_{\mathbf{k}} 2\delta(E - E_j(\mathbf{k})) = \frac{1}{4\pi^3}\int\limits_{E_j(\mathbf{k})=E} \frac{dS(\mathbf{k})}{|\nabla_{\mathbf{k}} E_j(\mathbf{k})|}, \quad (1)$$

where Ω is the volume of the solid, $E_j(\mathbf{k}) = E$ is the $\mathbf{k}$-space surface with constant energy E, and $\nabla_{\mathbf{k}} E_j(\mathbf{k})$ is the gradient of the energy dispersion, $S(\mathbf{k})$ means the smooth two dimensional surface, and $dS(\mathbf{k})$ represents the gradient of this surface. Within the parabolic band approximation (pba), this equation becomes

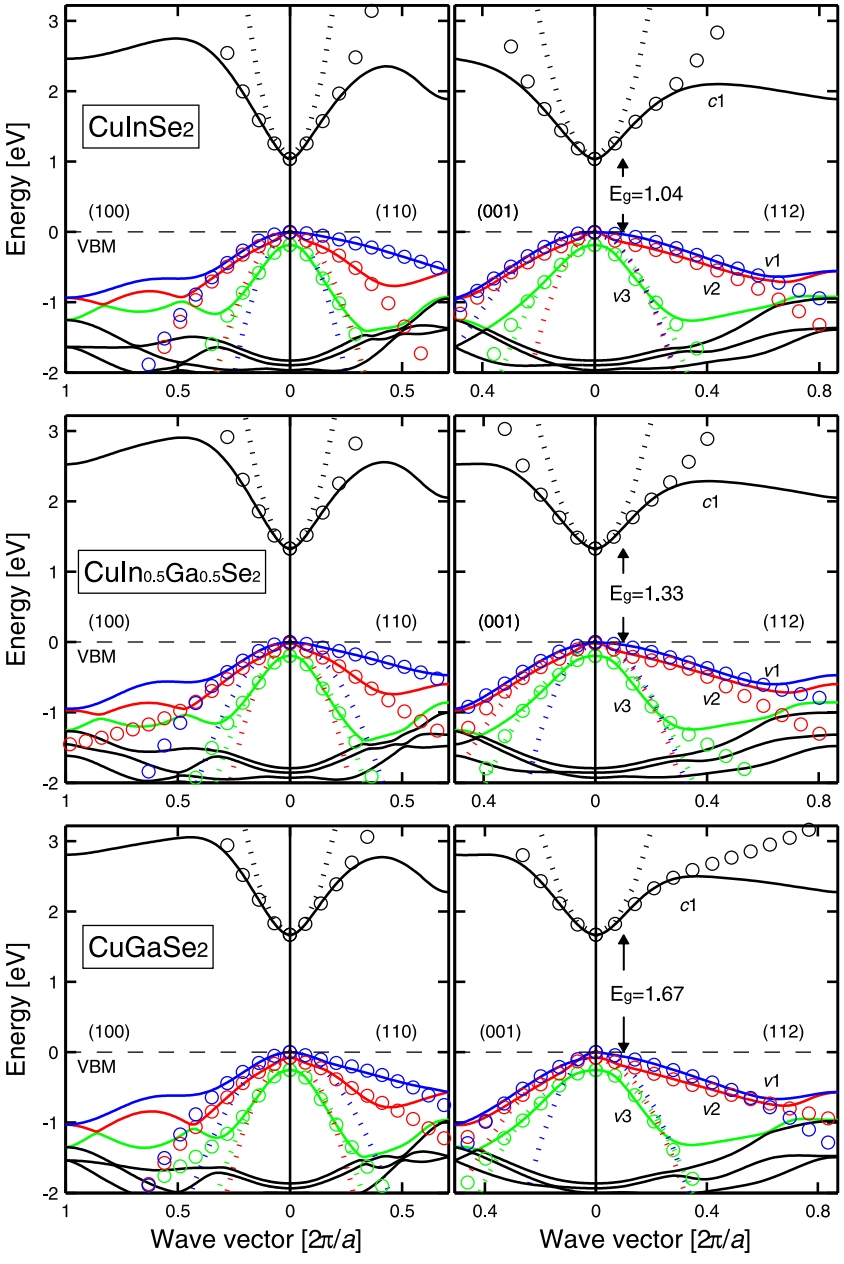

FIG. 1. Electronic band structure $E_j(\mathbf{k})$ of $CuInSe_2$ (upper panels), $CuIn_{0.5}Ga_{0.5}Se_2$ (middle panels), and $CuGaSe_2$ (lower panels) along four directions. The energies are referred to the VBM (dashed lines). Spin-orbit coupling is included, however, the notation of the energy bands ($j = v1$, $v2$, $v3$, and $c1$) refers to a spin-independent band indexing where $c1$ represents the lowest CB and $v1$ represents the topmost VB; these VBs are highlighted with colors in the online version. The solid lines show the full-potential results from Refs. 18 and 19, the circles are the results of the full band parameterization from Ref. 15, and the dotted lines represent the parabolic band approximation. Notice that the parabolic bands describe the two uppermost VBs poorly in the directions (100), (110), and (112).

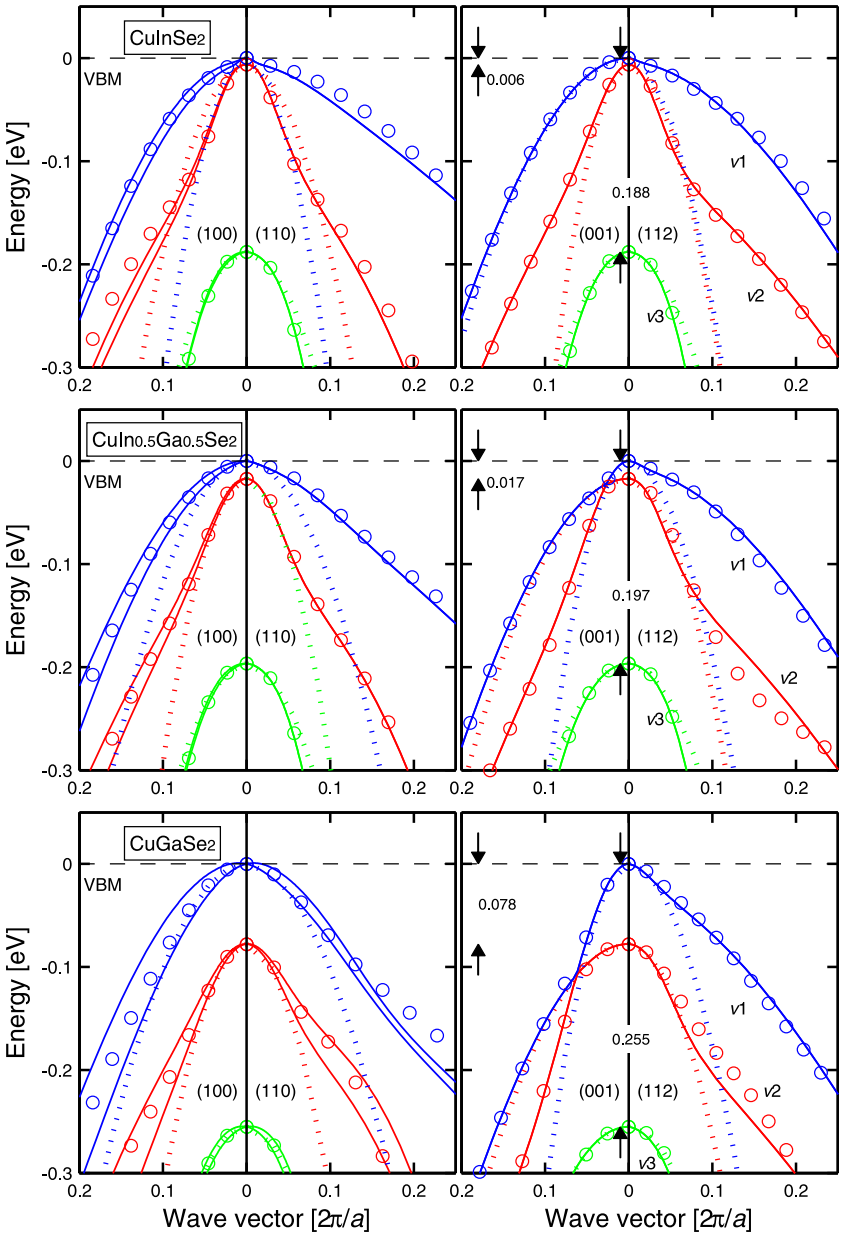

FIG. 2. Close-up of Fig. 1, demonstrating the strong non-parabolicity of the three uppermost VBs. Our parameterized energy bands $E_j(\mathbf{k})$ consider the average of the two spinor states $\psi_j^\sigma(\mathbf{k})$ with $\sigma = \downarrow$ and $\uparrow$, even though there is a relatively large split of the spin-up- and spin-down-like bands in the (100)-direction. This average approximation is justified by $\psi_j^\downarrow(-\mathbf{k}) = \psi_j^\uparrow(\mathbf{k})$, which overall make the material spin-independent. Therefore, the notation of the energy bands is $j = v1$, $v2$, and $v3$ refers to a spin-independent band indexing.

$$g_j^{pba}(E) = \frac{1}{2\pi^2}\left(\frac{2m_j^{DOS}}{\hbar^2}\right)^{3/2}\sqrt{|E - E_j(\mathbf{0})|}. \qquad (2)$$

Here, $E_j(\mathbf{0})$ is the band-edge energy, and the DOS mass $m_j^{DOS} = (m_j^\perp m_j^\perp m_j^\parallel)^{1/3}$ is a parameter that represents the capability of filling the specific band with free carriers to certain energy. For non-parabolic energy bands, Eq. (1) still holds, but the surface energy and the gradient of the energy dispersion are more complex. However, in order to utilize the simple and conventional form of the DOS (i.e., Eq. (2)), we define an energy-dependent DOS mass $m_{v/c}^{DOS}(E)$ as

$$g_{v/c}(E) = \sum_j g_j(E)$$

$$= \frac{1}{2\pi^2}\left(\frac{2m_{v/c}^{DOS}(E)}{\hbar^2}\right)^{3/2}\sqrt{|E - E_{v1/c1}(\mathbf{0})|}. \qquad (3)$$

With this definition to describe the full DOS, the energy-dependent DOS mass $m_{v/c}^{DOS}(E)$ will include the non-parabolicity and anisotropy of the band dispersion. The total DOS $g_{v/c}(E)$ is obtained by a summation over all relevant bands of the band-resolved DOS $g_j(E)$; in this work, we distinguishes between the total DOS of the valence bands $g_v(E)$ and the total DOS of the conduction bands $g_c(E)$.

B. The carrier concentration

The number of states $N_j(E)$ with energies up to E in the jth band is directly proportional to the $\mathbf{k}$-space volume enclosed by the constant energy surface $S_j(E)$. $N_j(E)$ is thus obtained by integrating $g_j(E)$ from $E_{v1/c1}(\mathbf{0})$ down/up to the energy E. In the case of band filling of free carriers with the concentration n, the constant energy surface is the Fermi energy $E_F(n)$.

The total concentration of free holes $n_v(T)$ in the valence bands and the total concentration of free electrons $n_c(T)$ in the conduction bands can be calculated from the DOS

$$n_v(T) = \int_{-\infty}^{E_{v1}(0)} g_v(E)(1-f(E))dE \text{ and}$$
$$n_c(T) = \int_{E_{c1}(0)}^{\infty} g_c(E)f(E)dE. \quad (4)$$

$f(E) = 1/[1+exp\{(E-E_F)/k_BT\}]$ is the temperature dependent Fermi distribution function where E_F is the Fermi energy and k_B is the Boltzmann constant. The intrinsic carrier concentration $n_i(T)$ can be determined from

$$n_i(T) = \sqrt{n_c(T) \cdot n_v(T)}, \quad (5)$$

whereas the extrinsic carrier concentration for p-type materials can be calculated from[20]

$$n_v(T) = \frac{n_i^2(T)}{n_v(T)} + \sum_{\alpha} \frac{N_{A_\alpha}}{1 + g_{A_\alpha} e^{(\Delta_{A_\alpha} - E_F)/k_BT}}. \quad (6)$$

Here, N_{A_α} is the acceptor concentration of the αth defect, Δ_{A_α} is the energy level of the acceptor state, and g_{A_α} is the spin-degeneracy factor. In this work, we assume two inequivalent acceptor levels in $CuIn_{1-x}Ga_xSe_2$ due to the presence of Cu vacancies V_{Cu}. The measured ionization energies for V_{Cu} are:[17] $E_A = 0.04$ eV and 0.06 eV for $CuInSe_2$, $E_A = 0.055$ eV and 0.08 eV for $CuIn_{0.5}Ga_{0.5}Se_2$, and $E_A = 0.06$ eV and 0.10 eV for $CuGaSe_2$. The value 0.08 eV for $CuIn_{0.5}Ga_{0.5}Se_2$ is an average estimate based on the values for $CuInSe_2$ and $CuGaSe_2$. Since the energy levels are very similar in the three compounds, we expect that the two acceptors states are equally populated.

III. RESULTS: INTRINSIC $CuIn_{1-x}Ga_xSe_2$

The electronic structure of the $CuIn_{1-x}Ga_xSe_2$ alloys ($x = 0$, 0.5, and 1) is presented in Figs. 1 and 2. The solid lines represent the results from the FPLAPW calculation. The full band parameterization refers to results based on parameterized energy dispersion[15] (circles in these figures), whereas the parabolic energy distribution (dotted lines) refers to the results based on energy bands with ellipsoidal shapes described by the Γ-point effective masses.[18,19] It is clear from Fig. 1 that parabolic bands are not accurate enough for neither the lowest CB (at least not for energies larger than 50–100 meV above the band gap) nor for the three uppermost VBs. Especially, the VBs are strongly non-parabolic. This is due to the fact that the crystal-field and spin-orbit interactions are strongly **k**-dependent. This is evident from Fig. 2, which shows the energy dispersion near the VB maximum, displaying non-parabolic band curvatures. The details in the curvatures of the topmost VBs and bottommost CB are related to the optical absorption in $CuIn_{1-x}Ga_xSe_2$. The absorption coefficient is relatively high in these chalcopyrites.[7,21] It is almost $3 \times 10^4\,cm^{-1}$ at a photon energy of 0.5 eV above the band-gap energy and this is, in part, a direct consequence of the flat character of the band-energy dispersion.

To further illustrate the non-parabolicity, the constant energy surfaces $S_j(E)$ are determined (Fig. 3) for the energies $E = 1$ meV (thus, $S_j(E)$ near the Γ-point; left column in the figure) and $E = 200$ meV ($S_j(E)$ away from the Γ-point; right column). Close to the Γ-point, the effective mass tensor is a proper parameter to represent the energy dispersion[18] in $CuIn_{1-x}Ga_xSe_2$, and thus the bands are in general ellipsoidal shaped there. For example, the effective masses for the topmost VB for $CuInSe_2$ are anisotropic ($m_{v1}^{\perp} = 0.14m_0$ and $m_{v1}^{||} = 0.66m_0$), so the constant energy surface is ellipsoidal in the vicinity of the Γ-point. The average value ($\sim 0.23m_0$) of the calculated hole masses is smaller than the measured value $m_{v1} \approx 0.7m_0$ in $CuInSe_2$ by Syrbu *et al.*[23] and Neumann *et al.*[24] Moreover, the effective hole mass in $CuGaSe_2$ [average value of $\sim 0.32m_0$ (Ref. 15)] has been estimated experimentally to be $m_{v1} \approx 0.64m_0$ by Luckert *et al.*[10] via magnetophotoluminescence measurements. Since the topmost VB is very non-parabolic, we expect that experimental results will yield a larger value if the measurements involves high hole concentration; see Sec. III A. Altogether, this indicates that the average hole mass at the Γ-point should be smaller than $\sim 0.7m_0$. The effective masses of the CB is however almost isotropic ($m_{c1}^{\perp} = 0.08m_0$ and $m_{c1}^{||} = 0.09m_0$ for $CuInSe_2$), so the corresponding constant energy surface is nearly spherical. These theoretical data for the effective electron mass are verified experimentally by Weinert *et al.*[25] $m_{c1} = 0.09m_0$ from Faraday rotation and also by Arushanov *et al.*[26] $m_{c1} = 0.08m_0$ from Shubnikov-de Haas oscillation results.

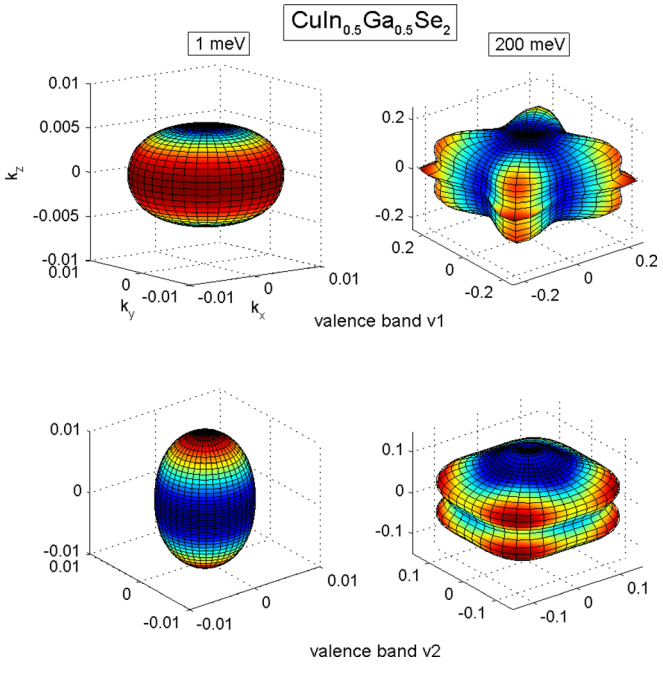

FIG. 3. Constant energy surfaces $S_j(E)$ for the two uppermost VBs in $CuIn_{0.5}Ga_{0.5}Se_2$ for the energies $E = 1$ meV (left column) and $E = 200$ meV (right column). The energy surfaces demonstrate that the VBs have ellipsoidal shapes in the vicinity of the Γ-point, but that they are very non-parabolic and anisotropic away from the Γ-point. In the supplementary information (Ref. 22), we present $S_j(E)$ for the CB, as well as corresponding results for $CuInSe_2$ and $CuGaSe_2$.

With an increasing distance from the Γ-point, the shape of the constant energy surfaces change. For the CB, the change is small. Also for the third uppermost VB (denoted $v3$ in the figure), the change is moderate. However, the changes of the constant energy surfaces for the two uppermost VBs ($v1$ and $v2$) are significant. For example, the topmost VB shows an extended energy surface in the (110) directions, which is a direct consequence of the very flat energy dispersion along that symmetry direction (cf. Fig. 2). One can, therefore, expect a larger concentration of free holes in these **k**-directions.

A. The DOS and the DOS masses

The total DOS of the VBs $g_v(E)$ and the total DOS of the CB $g_c(E)$ are presented in Fig. 4 for $CuIn_{1-x}Ga_xSe_2$. The difference between the parabolic approximation and the full parameterization of the bands is remarkable. This is true especially for the total DOS of the VBs, whereas the DOS of the CB indicates an ellipsoidal band curvature up to 50–100 meV above the band-gap energy. The full band parameterization generates always larger DOS, and this is a direct consequence from the fact that the overall band curvature is more flat than the curvature at the vicinity of the VB maximum and CB minimum. It is also evident that the VB DOS is much larger than the CB DOS for corresponding energy E (notice the different scales for DOS of the VB and the CB in the figure). The VB DOS of $CuGaSe_2$ is somewhat smaller than those of $CuInSe_2$ and $CuIn_{0.5}Ga_{0.5}Se_2$. The reason is that $CuGaSe_2$ has larger split-off energies of the second and third VBs (thus, $v2$ and $v3$ contribute less to the DOS in $CuGaSe_2$) and that $CuGaSe_2$ has a less flat topmost VB (thus, $v1$ has a smaller DOS in $CuGaSe_2$). The CB DOS of $CuGaSe_2$, however, is somewhat larger than those of $CuInSe_2$ and $CuIn_{0.5}Ga_{0.5}Se_2$ due to a more flat CB minimum.

From the total DOS and from the constant energy surfaces, the number of states with energies up to E is determined (Fig. 5). This quantity describes thus the carrier concentration due to external band filling of holes in the VBs and electrons in the CB for the given quasi-Fermi energies $E_{F,v}$* and $E_{F,c}$*, respectively, and at temperature $T = 0$ K. In agreement

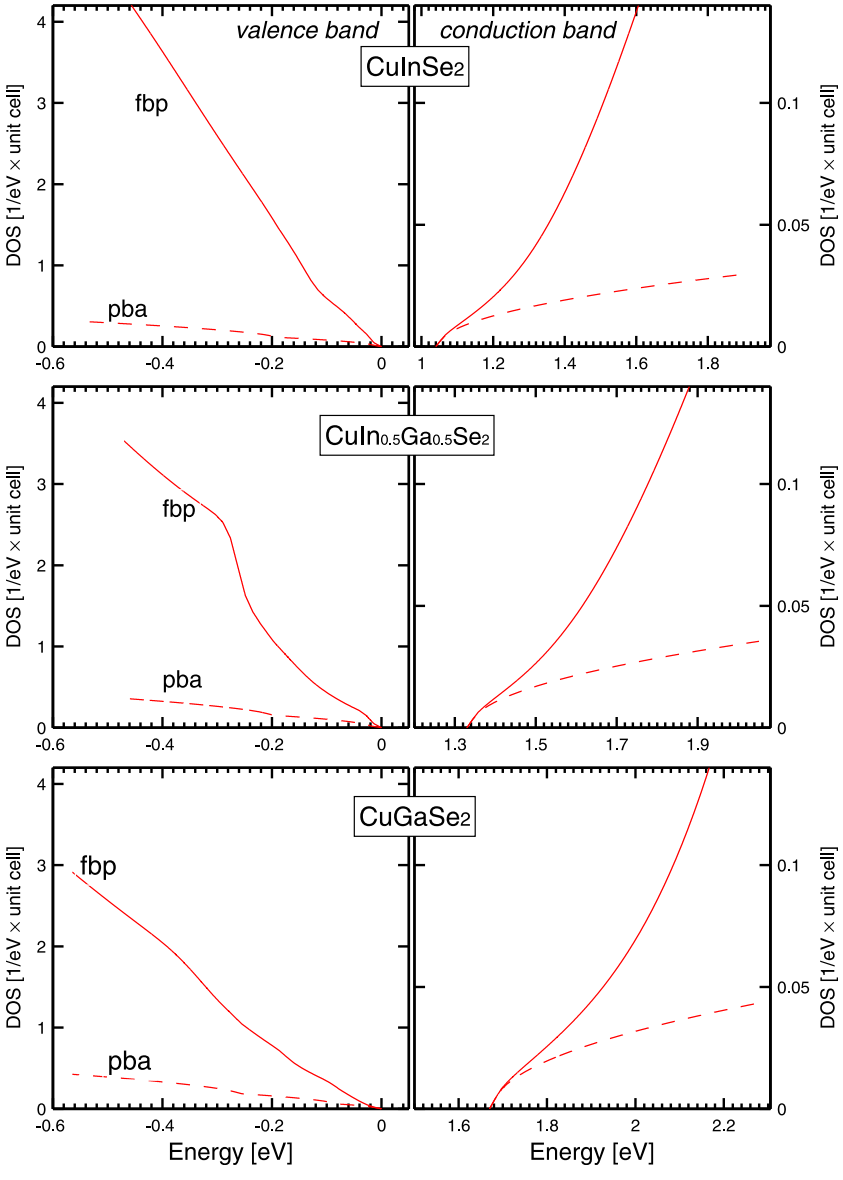

FIG. 4. Total DOS of the VBs (left panels) and of the CB (right panels) for $CuInSe_2$, $CuIn_{0.5}Ga_{0.5}Se_2$, and $CuGaSe_2$. The solid lines show the full band parameterization (fbp), and the dashed lines represent the parabolic band approximation (pba). The energies refer to the VBM. Notice the different scales in the figures for the VB and the CB. The results demonstrates that the non-parabolicity of the bands strongly affect the DOS dispersions.

with the discussion above for the total DOS, it is obvious that the VBs (CB) in Ga rich compounds will be less (more) populate by holes (electrons) for a given quasi-Fermi energy $E_{F,v}$* ($E_{F,c}$*). Thus, $CuGaSe_2$ can more easily host free electrons due to a more flat CB. However, a flat band implies heavier mass and thereby a weaker response to an applied electric field, which is negative for the electron transport.

Fig. 5 also demonstrates that the parabolic approximation of the bands strongly underestimates the band filling in the VBs and the CB. For example, the number of VB states of $CuInSe_2$ is increased by a factor of $\sim$18 at the positive energy $|\Delta E| = E_{v1}(\mathbf{0}) - E_{F,v}* = 0.1\,\text{eV}$ when the non-parabolicity is included, and for the corresponding CB, the number is increased by a factor of $\sim$3. At $|\Delta E| = 0.5\,\text{eV}$, the increase is as much as $\sim$41 and $\sim$8 times, respectively. This will have a strong impact on modeling band filling of especially holes for p-type $CuIn_{1-x}Ga_xSe_2$ materials.

In simulations and in analyses of measurements that involves free carrier concentrations, band filling of the energy bands is traditionally represented by the constant DOS mass (cf. Eq. (2)). This approach is valid for perfectly parabolic energy bands, but it is not an accurate description for $CuIn_{1-x}Ga_xSe_2$ with more complex energy dispersions (Figs. 1–3). In order to still use the traditional expression for

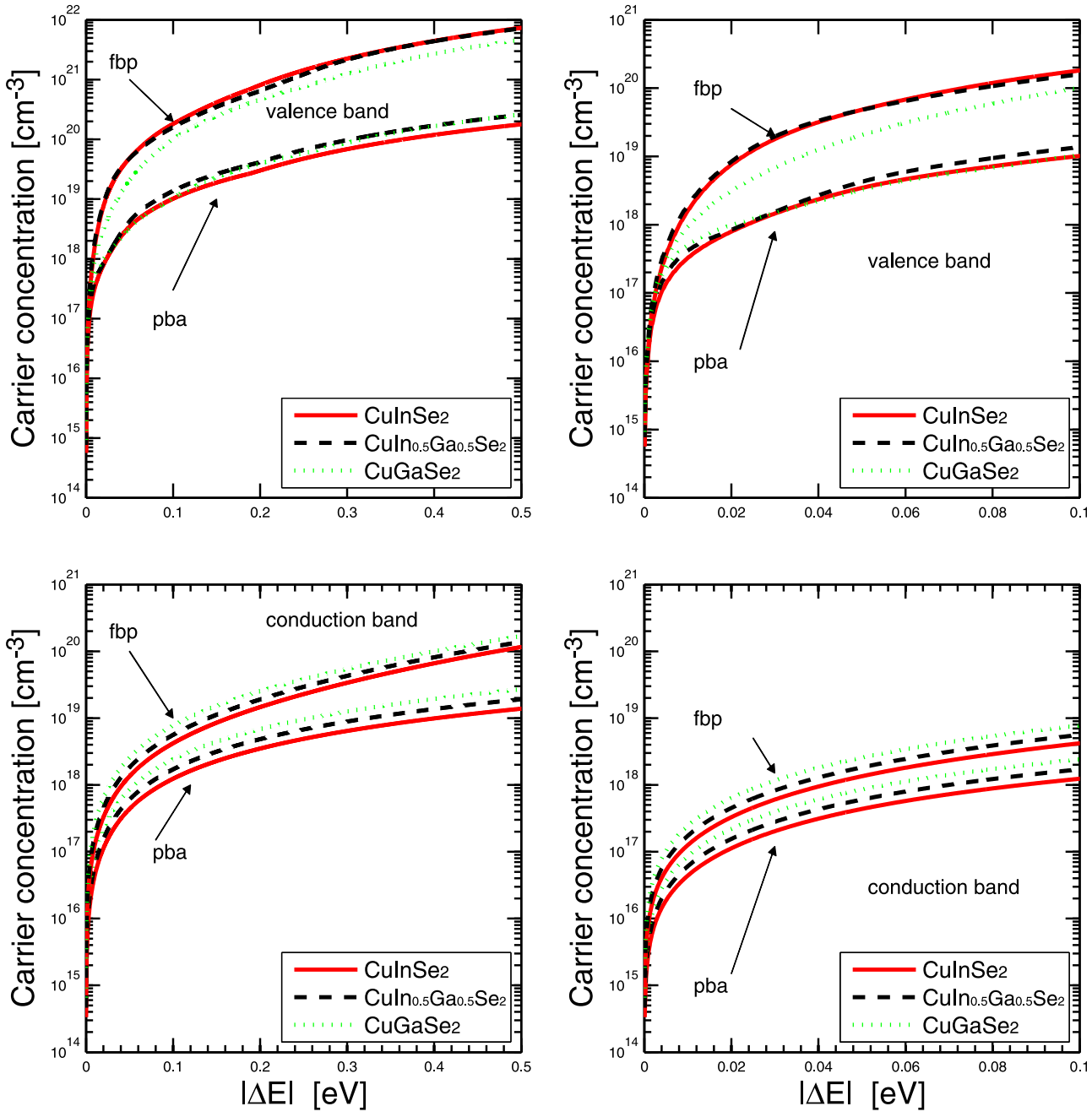

FIG. 5. Carrier concentration p or n as functions of the quasi-Fermi energy E_F* of the VBs $E_{F,v}$* and of the CB $E_{F,c}$*. Left column shows the results for large energy scale up to 0.5 eV, and right column displays a close-up for small Fermi energies. In the figure, $|\Delta E|$ is the positive energy difference $E_{v1}(\mathbf{0}) - E_{F,v}$* for the VBs and $E_{F,c}* - E_{c1}(\mathbf{0})$ for the CB. The carrier concentrations consider external band filling in intrinsic materials at $T = 0\,\text{K}$. The results demonstrate that the parabolic band approximation strongly underestimates the band filling of both the VBs and CB.

the DOS, we utilize the energy dependent DOS mass to model the DOS; see Eq. (3). The DOS masses for the $CuIn_{1-x}Ga_xSe_2$ (Fig. 6) show a very strong energy dependence of the VB DOS mass. This is directly related to the non-parabolicity and anisotropy of the VBs (cf. Fig. 2). For instance, the VB DOS masses in $CuInSe_2$ is $m_{v1}(E \approx 0) = (m_{v1}^{\perp} m_{v1}^{\perp} m_{v1}^{||})^{1/3} = 0.23 m_0$ in the vicinity of the Γ-point. This mass increases to $\sim 1.00 m_0$ when E is increased to ~ 0.1 eV. This may, therefore, explain the large measured hole masses $m_{v1} \approx 0.7 m_0$ in $CuInSe_2$ (Refs. 23 and 24) and $\sim 0.64 m_0$ in $CuGaSe_2$ (Ref. 10) since indirect measurements normally involves high hole concentrations.

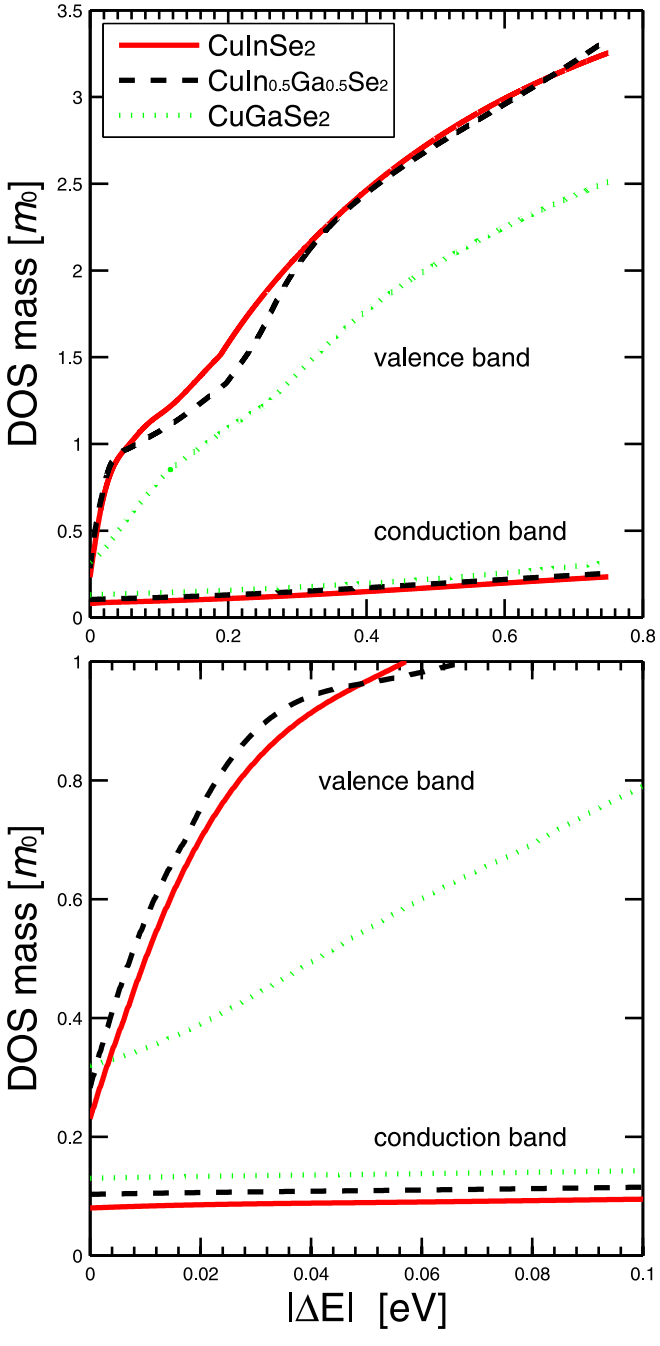

FIG. 6. The DOS mass $m_{v/c}^{DOS}(E)$ of the VBs and the CB in $CuInSe_2$, $CuIn_{0.5}Ga_{0.5}Se_2$, and $CuGaSe_2$. The upper (lower) panel shows $m_{v/c}^{DOS}(E)$ in a wider (narrower) energy region. This energy-dependent mass generates accurate quasi-Fermi energy $E_{F,v}$* and $E_{F,c}$* as function of the carrier concentration; see Eq. (3). |ΔE| is the energy difference $E_{v1}(\mathbf{0}) - E_{F,v}$* for the VBs and $E_{F,c}$* $- E_{c1}(\mathbf{0})$ for the CB; cf. Fig. 5.

The absolute change in the CB DOS mass is small, but the relative increase is 2–3 times with respect to the Γ-point value: $m_c^{DOS}(|\Delta E| = 0) = 0.080 m_0$, $0.103 m_0$, and $0.130 m_0$, whereas $m_c^{DOS}(|\Delta E| = 0.75\,\text{eV}) = 0.234 m_0$, $0.255 m_0$, and $0.316 m_0$, for $CuInSe_2$, $CuIn_{0.5}Ga_{0.5}Se_2$, and $CuGaSe_2$, respectively.

B. Temperature dependent band gap and Fermi level

The temperature dependency of the band-gap energy $E_g(T)$ is in this work modeled by empirical temperature dependence[27]

$$E_g(T) = E_g(0) - \frac{a \cdot T^2}{b + T}. \tag{7}$$

We use the experimental values for these parameters:[27,28] $E_g(0) = 1.04$ eV, $a = 1.086 \times 10^{-4}$ eV·K^{-1}, $b = 97$ K for $CuInSe_2$; $E_g(0) = 1.67$ eV, $a = 3 \times 10^{-4}$ eV·K^{-1}, $b = 277$ K for $CuGaSe_2$; $E_g(0) = 1.33$ eV, $a = 2.017 \times 10^{-4}$ eV·K^{-1} and $b = 209$ K for $CuIn_{0.5}Ga_{0.5}Se_2$. Here, the values of a and b for $CuIn_{0.5}Ga_{0.5}Se_2$ are estimated by averaging the data for $CuInSe_2$ and $CuGaSe_2$.

The band gap and the Fermi level of intrinsic $CuIn_{1-x}Ga_xSe_2$ are presented in Fig. 7(a). At temperature $T \approx 0$ K, the band gap is $E_g(0) = 1.04$, 1.33, and 1.67 eV for $x = 0$, 0.5, and 1, respectively, and the Fermi level is exactly the mid-gap energy $E_F(0) = E_g(0)/2$. With increasing temperature, the band gap is decreased as a consequence of the second term in Eq. (7). The corresponding Fermi level changes only slightly with temperature, but for $CuInSe_2$ and $CuIn_{0.5}Ga_{0.5}Se_2$, the Fermi levels increase somewhat more compared with $CuGaSe_2$. This is primarily due to the CB of DOS mass for $CuGaSe_2$ is almost the same, but the VB of DOS mass for $CuGaSe_2$ change smaller compared with $CuInSe_2$ and $CuIn_{0.5}Ga_{0.5}Se_2$ which will affect the DOS. As a consequence, the Fermi level is closer to the CB minimum in the In rich compounds. At $T = 300$ K and 600 K, the band-gap energies and Fermi energy are $E_g(300) = 1.02$, 1.29, and 1.62 eV, $E_g(600) = 0.98$, 1.24, and 1.55 eV, $E_F(300) = 0.55$, 0.69, and 0.84 eV, and $E_F(600) = 0.59$, 0.71, and 0.84 eV for $x = 0$, 0.5, and 1 respectively. The largest effect is thus seen for the Ga rich compounds, however the temperature effect is rather moderate (Table I).

C. Carrier concentration

The free carrier concentration (Fig. 7(b)) of intrinsic $CuIn_{1-x}Ga_xSe_2$ is calculated by considering the temperature dependency of the band gaps in Eq. (7). For comparison, we present also the results for Si and GaAs assuming parabolic energy dispersion. With increasing temperature, the carrier concentration is increased considerably. For instance, an increase of the temperature from 300 K to 600 K implies $\sim 10^5$ times higher carrier concentration in $CuInSe_2$. The small change in band gap and Fermi level as functions of temperature will have only small influence on the temperature dependence of carrier concentration. Instead, it is the temperature dependent Fermi distribution that governs the intrinsic carrier

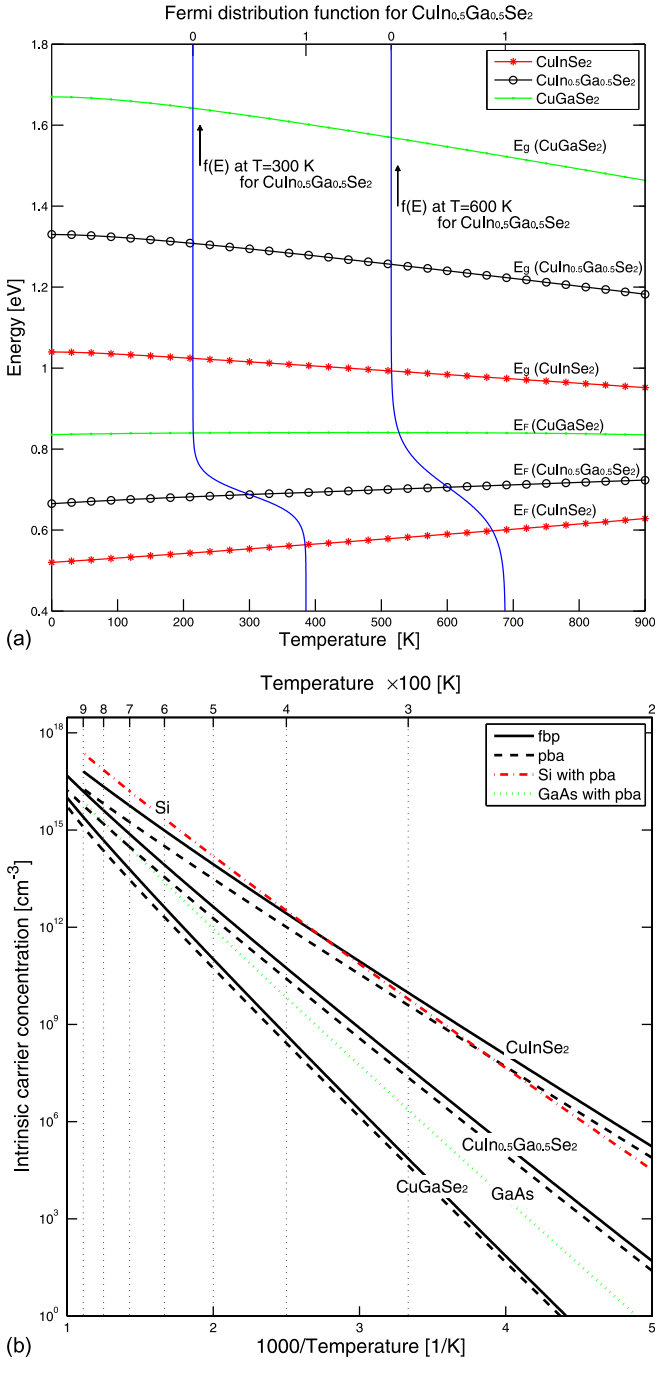

FIG. 7. (a) Band-gap energy E_g and Fermi energy E_F for $1 \le T \le 900$ K of intrinsic $CuInSe_2$, $CuIn_{0.5}Ga_{0.5}Se_2$, and $CuGaSe_2$, determined from the full band parameterization. In this figure, we also present the Fermi distribution $f(E)$ of $CuIn_{0.5}Ga_{0.5}Se_2$ for $T = 300$ K and 600 K. (b) Intrinsic carrier concentration as function of temperature. For comparison, the theoretical result for GaAs and Si using the parabolic band approximation is given.

concentration $n = p$ (see Fig. 7(b)). From the Fermi distribution of $CuIn_{0.5}Ga_{0.5}Se_2$, the probability of occupying the VB maximum (CB minimum) by a hole (an electron) is $\sim 3 \times 10^{-12}$ ($\sim 6 \times 10^{-11}$) at $T = 300$ K. The corresponding probability at $T = 600$ K is $\sim 1 \times 10^{-6}$ ($\sim 3 \times 10^{-5}$), and this relative increase of $\sim 10^6$ is directly seen in the temperature dependent carrier concentration.

Generally, at the same temperature, In rich compounds with small band gaps have higher carrier concentration

TABLE I. Γ-point energy gaps E_g, Fermi energies E_F with respect to the VB maximum, and free carrier concentrations $n = p$ in intrinsic $CuIn_{1-x}Ga_xSe_2$ ($x = 0$, 0.5, and 1) at temperature $T = 300$ K. Corresponding Fermi energies E_F^p and hole concentrations p are presented in p-type $CuIn_{1-x}Ga_xSe_2$ with effective acceptor concentrations of $N_A = 10^{17}$ and 10^{19} cm^{-3}. At $T \approx 0$ K, the band gap is $E_g = 1.04$, 1.33, and 1.67 eV for $x = 0$, 0.5, and 1, respectively.

	$CuIn_{1-x}Ga_xSe_2$		
	$x = 0$	$x = 0.5$	$x = 1$
Intrinsic			
E_g [eV]	1.02	1.29	1.62
E_F [eV]	0.55	0.69	0.84
$n = p$ [cm^{-3}]	1×10^{10}	5×10^{7}	7×10^{4}
$N_A = 10^{17}$ cm^{-3}			
E_F^p [eV]	0.138	0.137	0.126
p [cm^{-3}]	9×10^{16}	9×10^{16}	7×10^{16}
$N_A = 10^{19}$ cm^{-3}			
E_F^p [eV]	0.046	0.058	0.047
p [cm^{-3}]	3×10^{18}	2×10^{18}	1×10^{18}

compared with $CuGaSe_2$. This is due to a larger effect from the Fermi distribution function for materials with small energy gaps. One can notice from Fig. 7(b) that the free carrier concentration of $CuInSe_2$ (with the low-temperature band gap of $E_g = 1.04$ eV) is comparable with that of Si (with a similar gap of $E_g = 1.17$ eV). Also, the carrier concentration of GaAs (with $E_g = 1.52$ eV) lies between the carrier concentrations of $CuIn_{0.5}Ga_{0.5}Se_2$ ($E_g = 1.33$ eV) and $CuGaSe_2$ ($E_g = 1.67$ eV). Thus, the free carrier concentration of the intrinsic materials is strongly correlated to the band-gap energy. However, also the energy dispersion of the bands affects the carrier concentration. Taking into account the non-parabolicity of the band, the free carrier concentration is increased by a factor of 2 to 3.

The free carrier concentration in the intrinsic compounds is too small to affect the device performance; for example, $n = p \approx 1 \times 10^{10}$ cm^{-3} at 300 K and 3×10^{12} cm^{-3} at 400 K in $CuInSe_2$, which has the smallest band gap. Thus, dopants/defects with low activation energies are required for activate the semiconductor material.

IV. RESULTS: p-TYPE $CuIn_{1-x}Ga_xSe_2$

The determination of the Fermi level in p-type $CuIn_{1-x}Ga_xSe_2$ alloys is based on the band dispersion of the intrinsic materials, and by considering that the two inequivalent and shallow acceptor levels (see Sec. II B) are uncompensated. In addition to the temperature dependent band-gap energies $E_g(T)$ in Eq. (7) of the intrinsic materials, we also include a defect-induced narrowing of the gap according to Ref. 19. The resulting defect and temperature dependent band gap is then

$$E_g^p(T, N_A) = E_g(T) + \Delta E_{c1}(N_A) - \Delta E_{v1}(N_A). \quad (8)$$

Here, $\Delta E_{c1}(N_A)$ and $\Delta E_{v1}(N_A)$ are the energy shifts of the Γ-point CB minimum and VB maximum, respectively, due to the present of ionized acceptors with the concentration

N_A. We use the parameterized values of the energy shifts for p-type $CuIn_{1-x}Ga_xSe_2$ ($x=0$, 0.5, and 1) from Ref. 19

$$\Delta E_{c1}(N_A) = A_{c1}(N_A/10^{18})^{1/2} + B_{c1}(N_A/10^{18})^{1/4}$$
$$\Delta E_{v1}(N_A) = A_{v1}(N_A/10^{18})^{1/2} + B_{v1}(N_A/10^{18})^{1/4} + C_{v1}(N_A/10^{18})^{1/3}. \quad (9)$$

We use parameters from Ref. 19: $A_{c1}=-0.27$, -0.52, and -0.44 eV, $B_{c1}=-10.72$, -11.42, and -14.64 eV, $A_{v1}=7.16$, 20.87, and 13.26 eV, $B_{v1}=40.71$, 69.23, and 38.40 eV, and $C_{v1}=-25.11$, -67.11, and -26.66 eV, for $x=0$, 0.5, and 1, respectively. Apart from this acceptor-induced band-gap narrowing, we assume no effect on the host energy bands due to the presence of the shallow acceptors, although it is known that very high hole concentrations can affect the band dispersion[29] (still, the effective masses at the Fermi energy is almost unaffected).

A. Temperature dependent band gap and Fermi level

The calculated Fermi level E_F^P in p-type materials is presented in Fig. 8, referred to the Fermi level of the intrinsic materials E_F from Fig. 7(a). Only at very high temperatures ($T>400$ K) and for low acceptor concentrations, the Fermi level of p-type $CuIn_{1-x}Ga_xSe_2$ will reach the Fermi level of corresponding intrinsic compounds. Moreover, although the different compounds have comparable acceptor ionization energies, the Ga rich alloy has lower relative Fermi level; this is a direct consequence of the larger band gap of the Ga rich alloy.

By comparing the calculations with the parabolic band approximation (dotted lines in Fig. 8) and the full band approach (solid lines) for each of the three $CuIn_{1-x}Ga_xSe_2$ alloys, one can notice that the Femi level is similar for the two models only at low and at very high temperatures. In the mid-temperature region the difference is however apparent, especially for the high acceptor concentrations. Assuming parabolic bands yields always a lower Fermi level. The reason for this effect is that the energy dependent effective mass $m_{v/c}^{DOS}(E)$ in the full band parameterization is always larger that the corresponding Γ-point mass. Although the effect on the absolute value of the Fermi level seems to be small, it has an impact on the free carrier concentrations for highly doped materials.

B. Carrier concentration

The free carrier concentrations of p-type $CuIn_{1-x}Ga_xSe_2$ as functions of temperature and acceptor concentration are presented in Fig. 9. The carrier concentration can be divided into three regions: the freeze-out region for low temperatures, the extrinsic region in the mid-temperature region, and the intrinsic region at sufficiently high temperatures. For example, consider $CuInSe_2$ with the acceptor concentration $N_A=10^{13}\,cm^{-3}$ in Fig. 9. At very low temperatures ($T<100$ K), part of the host electrons are excited to the acceptor-like states whereas remaining host electrons are "frozen." With an increase of the temperature, more and more electrons in the VBs are thermally excited, until all acceptor states are occupied. The calculated concentrations in this region are in fairly good agreement with experimental carrier concentrations from low-temperature Hall mobility measurements by Schroeder *et al.*[9] Both the calculated and measured data indicate that the freeze-out region is as high as room-temperature even for moderately doped $CuInSe_2$ ($N_A\approx 10^{17}$–$10^{18}\,cm^{-3}$).

With a further increase of the temperature, the free carrier concentration will be constant for a wide temperature range; this is the extrinsic region. When the temperature is increase even further, the free carrier concentration will be enhanced due to electron excitation across the band gap as for the intrinsic materials.

From the figure, one can observe that the transition from the freeze-out region to the extrinsic region occurs well below the room temperature unless the uncompensated acceptor concentration is above $\sim 10^{18}\,cm^{-3}$. Due to the slightly lower ionization energies for the In rich compounds, these compounds have lower temperature for the transition to the extrinsic region. For high uncompensated acceptor concentrations (i.e., $>10^{18}\,cm^{-3}$), not all acceptors are ionized at room temperature (see Table I). Moreover, since the In rich compounds also have smaller band gaps, the transition from the extrinsic region to the intrinsic region occurs at lower temperatures for these compounds.

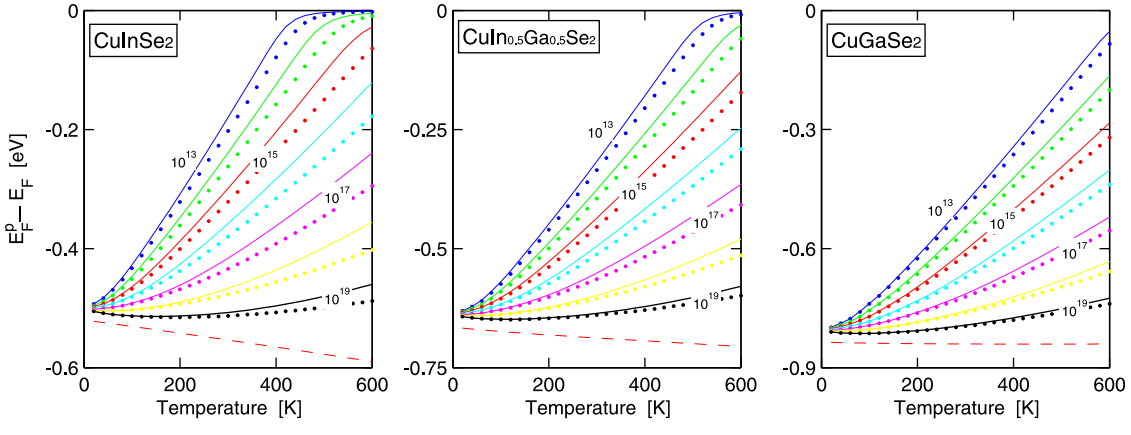

FIG. 8. Fermi level as function of the temperature $20\le T\le 600$ of p-type $CuInSe_2$, $CuIn_{0.5}Ga_{0.5}Se_2$, and $CuGaSe_2$ for the effective doping concentration $N_A=10^{13}$, 10^{14}, 10^{15}, …, and 10^{19} acceptors/cm^3. The energy scale $E_F{}^p-E_F$ describes the Fermi energy with respect to the intrinsic E_F; see Fig. 7. Dashed lines represent the VBM with respect to the intrinsic Fermi level. Solid and dotted lines represents the full band parameterization and the parabolic band approximation, respectively.

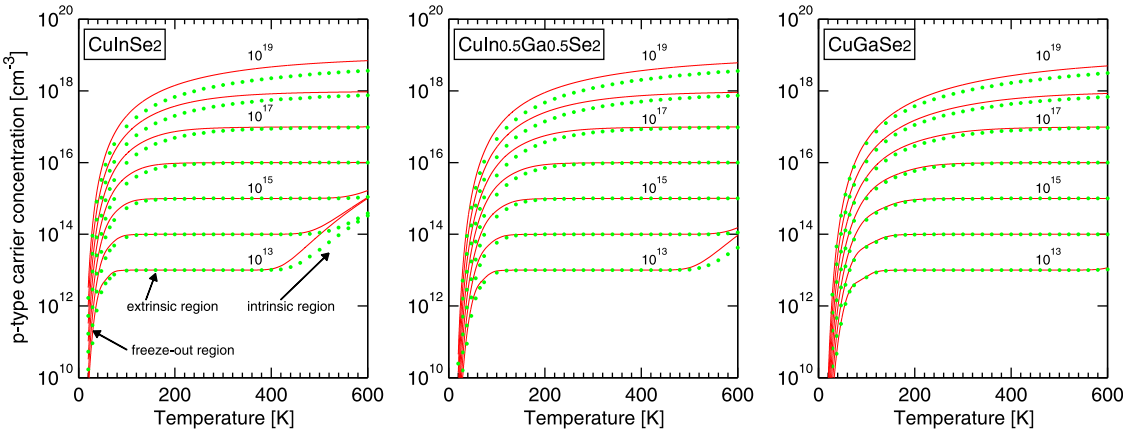

FIG. 9. Free carrier concentration as function of the temperature in p-type $CuInSe_2$, $CuIn_{0.5}Ga_{0.5}Se_2$, and $CuGaSe_2$ for the effective doping concentration $N_A = 10^{13}$, 10^{14}, 10^{15},..., and 10^{19} acceptors/cm^3. Solid and dotted lines represents the full band parameterization and the parabolic band approximation, respectively. The full band description of the energy dispersion is important for high doping concentrations and/or in the intrinsic region for cross-gap excitations at high temperatures.

The intrinsic region is however only important for very low acceptor concentrations.

By comparing the results from the parabolic band approximation and from the full band parameterization for each compound, one can observe that the approximation underestimates the free carrier concentrations roughly by a factor of 2 in both the freeze-out region and also in the intrinsic regions. Due to this underestimate, the transition from freeze-out to extrinsic regions tends to occur at a somewhat higher temperature for the approximated method, and also the transition from the extrinsic to the intrinsic region also at a somewhat higher temperature. Although the carrier concentration is fully described in the extrinsic region by assuming parabolic bands since all acceptors are ionized, the Fermi level is not well described within this approximation (see Fig. 8). Thus, in order accurately describe the free carrier concentration as well as its temperature dependency, a full description of the energy dispersions is needed.

V. SUMMARY

To summarize, we have analyzed the energy band dispersion and the carrier concentration in chalcopyrite $CuIn_{1-x}Ga_xSe_2$ ($x = 0$, 0.5, and 1) alloys. The overall results are: (i) the three uppermost VBs are strongly anisotropic and non-parabolic. (ii) The lowest CB becomes non-parabolic for energies 50–100 meV above the Γ-point band minimum. (iii) A constant DOS mass cannot accurately describe band filling of the VBs even at low hole concentrations. Instead, we introduce an energy dependent DOS mass that can be utilized to describe the carrier concentration and the Fermi energy using traditional equations for the DOS. (iv) With the full description of the energy dispersion, the hole concentration is improved by a factor of 10–50 and the electron concentration is improved by a factor of 2–10 depending on quasi-Fermi energy. (v) The transition from the freeze-out region to the extrinsic region occurs well below the room temperature for uncompensated acceptor concentration below $\sim 10^{17}\,\mathrm{cm}^{-3}$, whereas for higher concentrations, not all acceptors are ionized at $T = 300\,\mathrm{K}$.

Thus, with a more correct description of the energy dispersions, one can better analyze the electron and hole dynamics in the $CuIn_{1-x}Ga_xSe_2$ alloys, thereby better understand the electrical properties of these compounds.

ACKNOWLEDGMENTS

This work is supported by the China Scholarship Council, the Swedish Energy Agency, and the Swedish Research Council. We acknowledge access to high-performance computing resources at the NSC and HPC2N centers through SNIC/SNAC and Matter network.

[1]M. D. Archer and R. Hill, *Clean Electricity from Photovoltaics* (Imperial, London, 2001).
[2]V. Nadenau, U. Rau, and H. W. Schock, J. Appl. Phys. **87**, 584 (2000); A. Jasenek, U. Rau, V. Nadenau, and H. W. Schock, J. Appl. Phys. **87**, 594 (2000).
[3]S. R. Kodigala, *Cu(In$_{1-x}$Ga$_x$)Se$_2$ Based Thin Film Solar Cells* (Elsevier, Burlington, MA, 2010), Vol. 35.
[4]R. Noufi, R. Axton, C. Herrington, and S. K. Deb, Appl. Phys. Lett. **45**, 668 (1984).
[5]S. Ishizuka, H. Shibata, A. Yomada, P. Fons, K. Sakurai, K. Matsubara, S. Niki, M. Yonemura, and H. Nakanishi, J. Appl. Phys. **100**, 096106 (2006).
[6]Y.-J. Zhao, C. Persson, S. Lany, and A. Zunger, Appl. Phys. Lett. **85**, 5860 (2004).
[7]I. Mártil, J. Santamaria, G. Gonzalez-Diaz, and F. Sanchez-Quesada, J. Appl. Phys. **68**, 189 (1990).
[8]E. Arushanov, S. Siebentritt, T. Schedel-Niedrig, and M. C. Lux-Steiner, J. Appl. Phys. **100**, 063715 (2006).
[9]D. J. Schroeder, J. L. Hernandez, G. D. Berry, and A. A. Rockett, J. Appl. Phys. **83**, 1519 (1998).
[10]F. Luckert, M. V. Yakushev, C. Faugeras, A. V. Karotki, A. V. Mudryi, and R. W. Martin, Appl. Phys. Lett. **97**, 162101 (2010).
[11]M. A. Mannan, M. S. Anjan, and M. Z. Kabir, Solid-State Electron. **63**, 49 (2011).
[12]S. A. Dinca, E. A. Schiff, B. Egaas, R. Noufi, D. L. Young, and W. N. Shafarman, Phys. Rev. B **80**, 235201 (2009).
[13]S. H. Han, F. S. Hasoon, A. M. Hermann, and D. H. Levi, Appl. Phys. Lett. **91**, 021904 (2007).
[14]A. Hofmann and C. Pettenkofer, Phys. Rev. B **84**, 115109 (2011).
[15]R. Chen and C. Persson, Thin Solid Films **519**, 7503 (2011).
[16]J. M. Luttinger and W. Kohn, Phys. Rev. **97**, 869 (1955); G. Dresselhaus, A. F. Kip and C. Kittel, Phys. Rev. **98**, 368 (1955); E. O. Kane, J. Phys. Chem. Solids **1**, 82 (1956).
[17]S. Siebentritt, M. Igalson, C. Persson, and S. Lany, Prog. Photovolt: Res. Appl. **18**, 390 (2010).

[18]C. Persson, Appl. Phys. Lett. **93**, 072106 (2008).
[19]C. Persson, Thin Solid Films **517**, 2374 (2009).
[20]S. M. Sze, *Semiconductor Devices: Physics and Technology*, 2nd ed. (Wiley, Toronto, 2002).
[21]M. I. Alonso, K. Wakita, J. Pascual, M. Garriga, and N. Yamamoto, Phys. Rev. B **63**, 075203 (2001); N. K. Hönes, M. Eickenberg, S. Siebentritt, and C. Persson, Appl. Phys. Lett. **93**, 092102 (2008); S.-H. Han, C. Persson, F. S. Hasoon, H. Al-Thani, A. M. Hermann, and D. Levi, Phys. Rev. B **74**, 085212 (2006).
[22]See supplementary material at http://dx.doi.org/10.1063/1.4767120 for constant energy surfaces in $CuInSe_2$, $CuIn_{0.5}Ga_{0.5}Se_2$, and $CuGaSe_2$.
[23]N. N. Syrbu, I. M. Tiginyanu, L. L. Nemerenco, V. V. Ursaki, V. E. Tezlevan, and V. V. Zalamai, J. Phys. Chem. Solids **66**, 1974 (2005).
[24]H. Neumann, W. Kissinger, H. Sobotta, V. Riede, and G. Kühn, Phys. Status Solidi B **108**, 483 (1981).
[25]H. Weinert, H. Neumann, H.-J. Höbler, G. Kühn, and N. van Nam, Phys. Status Solidi B **81**, K59 (1977).
[26]E. Arushanov, L. Essaleh, J. Galibert, J. Leotin, M. A. Arsene, J. P. Peyrade, and S. Askenazy, Appl. Phys. Lett. **61**, 958 (1992).
[27]*Landolt-Börnstein: Numerical Data and Functional Relationships in Science and Technology*, edited by O. Madelung *et al*., New Series, Group III, Vol. 17h (Springer, Berlin, 1985).
[28]H. Neumann, W. Hörig, E. Reccius, W. Möller, and G. Kühn, Solid State Commun. **27**, 449 (1978).
[29]C. Persson, B. E. Sernelius, A. Ferreira da Silva, R. Ahuja, and B. Johansson, J. Phys. Condens. Matter **13**, 8915 (2001).